J. Biochem. 2009;145(1)67–77
doi:10.1093/jb/mvn141

Spectroscopic Studies on the Comparative Interaction of Cationic Single-Chain and Gemini Surfactants with Human Serum Albumin

Nuzhat Gull[1], Priyankar Sen[2], Rizwan Hasan Khan[2] and Kabir-ud-Din[1,*]

[1]Department of Chemistry; and [2]Interdisciplinary Biotechnology Unit, Aligarh Muslim University, Aligarh 202 002, India

Received September 17, 2008; accepted October 18, 2008; published online October 30, 2008

To gain insights into the comparative effect of single-chain/gemini surfactants on proteins and the possible implications, the interaction of human serum albumin (HSA) with cationic single-chain surfactant cetyltrimethylammonium bromide (CTAB) and its gemini counterpart *bis*(cetyldimethylammonium)butane dibromide with spacer –$(CH_2)_4$– (designated as G4) using turbidity measurements, far-UV and near-UV circular dichroism (CD), intrinsic fluorescence and extrinsic fluorescence spectroscopy at pH 7.0 are reported in this contribution. A decrease of 33.5% α-helical content at 22.5 μM G4 was monitored compared to a 15% decrease at 2,250 μM CTAB. Against a 3.5% increase at 11,250 μM CTAB, a rise of 21.1% in the α-helical content was observed 375 μM G4. The result is related to the stronger electrostatic and hydrophobic forces in G4, owing to the presence of two charged headgroups and two hydrophobic hydrocarbon tails that make it to bind strongly to the protein compared to its single chain counterpart, CTAB, resulting in larger unfolding. The stabilization at higher concentrations is attributed to the highly hydrophobic microdomain of the G4 aggregates formed at such concentrations. The results of the multi-technique approach are consistent with the fact that the gemini surfactants are more efficient than their conventional single-chain counterparts and hence may be used more effectively in the renaturation of proteins produced in the genetically engineered cells via the artificial chaperone protocol, as solubilizing agents to recover proteins from insoluble inclusion bodies and in drug delivery.

Key words: aggregation, circular dichroism, gemini surfactants, human serum albumin, fluorescence spectroscopy.

Abbreviations: CTAB, cetyltrimethylammonium bromide; HAS, Human serum albumin; RFI, relative fluorescence intensities.

INTRODUCTION

Proteins are the most abundant and versatile macromolecules in living systems and serve crucial functions in essentially all biological processes. The function of a protein is directly dependent on its three-dimensional structure. The protein–surfactant interactions have been the subject of extensive research (*1*, *2*) ever since surfactants were found to be strong denaturants of water soluble proteins (*3*). Denaturation of proteins by ionic surfactants involves binding of the surfactant ions to sites on the protein molecules, which occurs at 1–3 mmol dm^{-3} surfactant concentration (*4*). This concentration range is much lower than that required for other commonly used denaturants such as urea (6–8 mol dm^{-3}) or GdmCl (4–6 mol dm^{-3}), wherein the denaturing process primarily depends on the effect of these compounds on the water structure and weakening of the hydrophobic interactions in the tertiary structure of the proteins (*5–7*). The understanding of protein folding/unfolding has not only provided an intellectual challenge but also has an immense potential for application. Besides shedding light on the functional properties of the proteins, the protein–surfactant interactions are significant for wide variety of industrial, biological, pharmaceutical and cosmetic systems (*1*, *2*, *8–16*).

The energetics of protein conformation appears to be driven by the hydrophobic effect (*17*) or the degree of attraction for water (*18*). Due to the hydrophobic and hydrophilic properties of the amino acids, a protein exhibits dualism that makes small amphiphilic molecules to interact with proteins. The amphiphilic molecules chosen to study the protein–surfactant complexes, in general, are the ionic surfactants in view of their application in the area of membrane studies (*19*, *20*). The role of surfactant polar head structure in the protein–surfactant complexation was examined by Moore *et al*. (*21*). The formation of complexes between anionic surfactants and proteins in aqueous solutions has been well established (*22–26*). Cationic surfactants have been found to interact with the proteins to a lesser extent compared to anionics mainly as a consequence of smaller relevance of electrostatic interactions at the pH's of interest.[27] However, the binding isotherms of both these type of surfactants have

*To whom correspondence should be addressed. Tel: +91-571-2703515 Extn. 3353, Fax: 0091-571-2708088,
E-mail: kabir7@rediffmail.com

been found to be similar (*27*, *28*). The conformational changes induced in the protein, when the surfactant binds to it, result in changes of polarity and the stability of the protein (*22*, *23*, *29*, *30*).

A novel class of surfactants called 'Gemini surfactants' has been developed in the recent years. These surfactants are made up of two hydrophobic chains and two polar headgroups covalently linked through a spacer group (*31*, *32*). These surfactants possess properties such as low Kraft temperature, low cmc, strong hydrophobic microdomain, etc., that make them superior to conventional monomeric surfactants (*33*). They can be orders of magnitude more surface active than the comparable conventional surfactants (*34*). Geminis have already shown promise in various potential areas of surfactant application. Referred to as 'second generation surfactants' they are being intensely investigated (*35*, *36*).

Although a large amount of work has been done on the interaction of single-chain ionic surfactants with proteins, gemini surfactant–protein interactions are less studied (*37–40*). This communication details a comparative interaction of cetyltrimethylammonium bromide (CTAB), $C_{16}H_{33}N^+(CH_3)_3Br^-$ and its gemini counterpart with spacer chain $-(CH_2)_4-$, $C_{16}H_{33}(CH_3)_2N^+-(CH_2)_4-N^+(CH_3)_2C_{16}H_{33}2Br^-$, on human serum albumin (HSA–a globular protein), using UV-visible spectroscopy, intrinsic fluorescence, extrinsic fluorescence and circular dichroism. Keeping in view the special interest in the effect of surfactants on humans, particularly in pharmaceutical, biotechnological and the cosmetic industry, HSA was selected as the model protein. The structure of HSA has been determined to a resolution of 2.8 Å (*41*). HSA is single polypeptide chain, multi-domain protein composed of 585 amino-acid residues (*42*). It consists of three homologous domains that ensemble to form a heart-shaped molecule. Each domain in turn is the product of subdomains A and B which are extensively cross-linked by disulphide bridges. There are 10 principal helices in each domain, h1–h6 for subdomain A and h7–h10 for subdomain B. Helped by 17 disulphide bridges, the protein is folded into a shape that can be roughly described by an equilateral triangle with sides of about 80 Å and thickness of about 30 Å (*43*). At neutral pH, it has a net negative charge (pI 5.2) and is known to undergo conformational changes at both low and high pH's (*44*). It aids in the transport, metabolism and distribution of exogenous and endogenous ligands. It serves to maintain the plasma pH, contributes to colloidal blood pressure, functions as carrier of many metabolites of fatty acids and serves as a major transport protein in plasma (*45*).

MATERIAL AND METHODS

Material—Human serum albumin (HSA) essentially fatty acid free (lot no. 3872A, Sigma), cetyltrimethylammonium bromide (CTAB, Sigma), 1-anilino-8-naphthalene sulphonic acid (ANS, Sigma) were used as received. The gemini *bis*(cetyldimethylammonium)butane dibromide ($C_{16}H_{33}(CH_3)_2N^+-(CH_2)_4-N^+(CH_3)_2\ C_{16}H_{33}\cdot 2Br^-$, G4) was synthesized and characterized as described elsewhere (*33*). All other reagents and buffer components used were of analytical grade. Double distilled water was used throughout the study. Stock solutions of extensively predialysed HSA, CTAB and G4 were prepared in 20 mM sodium phosphate buffer (pH 7) and utilized to prepare the samples of desired concentrations. Compared to a critical micellar concentration (cmc) of 1 mM for CTAB and 28 μM for G4 the cmc in the sodium phosphate buffer (pH 7) was determined to be 0.634 mM and 15 μM for CTAB and G4, respectively, by using the concentration of HSA used for the measurements carried out was 7.5 μM. Proteins concentrations were determined from the value of specific extinction coefficient ($\epsilon^{1\%}_{1\,cm} = 5.3$) by measuring the absorbance of protein solutions at 280 nm on a Hitachi U-1,500 spectrophotometer (*46*), model U-1500 or alternately by method of Lowry *et al*. (*47*). The concentration of the ANS used for extrinsic fluorescence measurements was 50 times that of the protein and was determined from the value of the extinction coefficient $5.000\ M^{-1}cm^{-1}$ by measuring the absorbance of the solution at 350 nm. The pH measurements were carried out on an ELICO digital pH meter (model LI610).

Turbidity Measurements—The turbidity of the surfactant/HSA solutions was monitored by UV absorbance at 350 nm using a Shimadzu UV/vis spectrometer. A cuvette with 1 cm path length was used. The measurements were carried out at 25°C. A reference sample containing buffer and the detergent was measured and the absorbance observed was negligible.

CD Measurements—CD measurements were carried out with a Jasco spectropolarimeter, model J-720, equipped with a microcomputer. The instrument was calibrated with D-10-camphorsulfonic acid. All the CD measurements were carried out at 25°C with a thermostatically controlled cell holder attached to a Neslab RTE-110 water bath with an accuracy of ±0.1°C. The high-tension voltage for the spectra obtained was found to be less than 600 V. Spectra were collected with a scan speed of 20 nm/min and response time of 1 s. Each spectrum was the average of four scans. A reference sample containing buffer and the detergent was subtracted from the CD signal for all measurements. Far-UV and near-UV CD spectra were measured at protein concentration of 7.5 μM. The path length was 1 mm and 1 cm, respectively. The results were expressed as mean residue ellipticity (MRE) in deg cm^2 $dmol^{-1}$, defined as

$$MRE = \frac{\theta_{obs}}{10 \times n \times C_p \times l}.$$

The α-helical content was calculated from the MRE values at 222 nm using the following equation (*48*),

$$\text{Percentage of } \alpha\text{-helix} = \left(\text{MRE}_{222\,nm} - \frac{2{,}340}{30{,}300}\right) \times 100$$

where θ_{obs} is the CD in millidegree, n is the number of amino-acid residues (585), l is the cell-path length in cm and C_p the molarity.

Fluorescence Measurements—Fluorescence measurements were performed on a Hitachi spectrofluorimeter (model 2500) equipped with a PC. The fluorescence spectra were collected at 25°C with a 1 cm path length cell. The excitation and emission slits were set at 5 nm. The fluorescence spectra were taken with a protein concentration of 7.5 μM. To the 7.5 μM protein stock

solution, different volumes of the buffer were added followed by the requisite volumes of stock additive solutions to obtain samples of the desired additive concentration. The reference sample consisting of the buffer and the detergent didn't give any fluorescence signal. Intrinsic fluorescence was measured by exciting the protein solution at 280 nm and 295 nm and emission spectra were recorded in the range of 300–400 nm.

For extrinsic fluorescence measurements in the ANS binding studies, the excitation was set at 380 nm and the emission spectra were taken in the range of 400–600 nm or at a fixed wavelength of 470 nm.

RESULTS AND DISCUSSION

Aggregation Studies—The protein–surfactant mixed solutions are transparent throughout the investigated concentration range in case of CTAB. The HSA–G4 mixed solutions are clear at low surfactant concentrations; turbidity appears in the solutions with rising G4 concentration and increases so much so that the samples turn opaque. With further addition of the surfactant the turbidity again shows a decreasing trend and finally disappears. The fluctuations in turbidity arise mainly from the change in the amount and size of aggregates formed and is attributed to the formation and redissolution of HSA–surfactant complexes (*49–51*). These changes are tracked by following the variations in the absorbance of the HSA–cationic surfactant mixed solutions at 350 nm employing UV-visible spectroscopy.

The comparative effect of CTAB/G4 on the UV-absorbance of HSA at 350 nm is illustrated in Fig. 1. The variation in turbidity observed when CTAB is added to the protein is negligibly small compared to the changes monitored on the addition of G4. The very small change in the absorbance values of the HSA–CTAB mixed solutions compared to the native protein is attributed to the fact that the cationic surfactants exhibit a low tendency to interact with proteins (*1*, *52*). An increase in the absorbance of HSA–G4 mixed solutions is observed as the surfactant is added to the protein; it decreases with increasing surfactant concentration and attains a constant value finally. The results suggest that the HSA–G4 interactions are stronger compared to the interactions of the protein with CTAB.

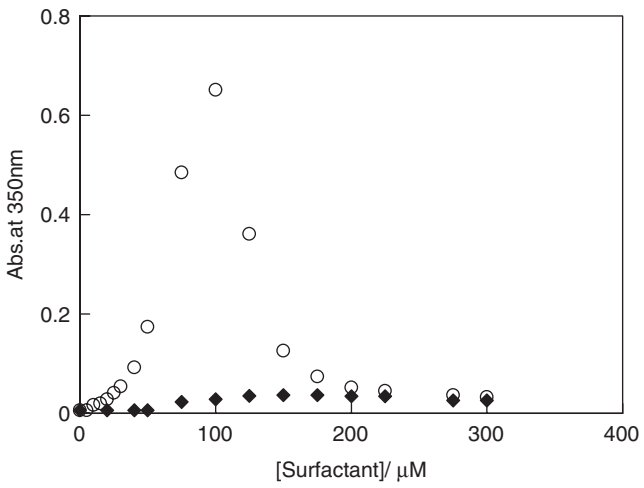

Fig. 1. **Turbidity curves for HSA (7.5 μM) at pH 7 with the varying concentrations of CTAB (filled diamond) and G4 (filled circle) (temp. 25°C).**

To have insights into the interactions and to interpret them more meaningfully, CD and fluorescence spectroscopy is employed. Only the clear samples with low absorbance were used for such studies as the turbid samples with insoluble aggregates could not be studied since these cause artifacts due to (i) differential light scattering which arises when light falls on chiral particles of dimensions comparable to or greater than its wavelength, and (ii) absorption flattening which arises from the high concentration of the proteins in such aggregates.

Far-UV CD—Alterations of ellipticity at 222 nm ($-MRE_{222}$) are useful probe for visualizing varying α-helical contents.[48] Therefore, circular dichroism (CD) measurements were performed to monitor the changes of the secondary structure generated by the interaction of HSA with CTAB or G4.

Typical far-UV CD spectra in the range 200–250 nm for native HSA and HSA in the presence of surfactants are shown in the Fig. 2. The spectrum of untreated HSA at pH 7 shows negative minima nearly at 208 nm and 222 nm, characteristic of α-helical structure (*53*). It is observed that when CTAB is added to HSA (Fig. 2A and Table 1), the mean residue ellipticity ($-MRE_{222}$) and hence the α helical content, as calculated by the method of Chen (*48*), decreases from 58.2% when untreated to 41.5% at a surfactant concentration of 2,250 μM, increases again to 45% at 11,250 μM CTAB, and assumes an almost constant value thereafter. The α-helical content in G4 decreases from 58.2% (in the untreated state) to 24.7% at 22.5 μM surfactant concentration. Afterwards, the helical content begins to rise and attains a value of 45.8% at 375 μM, remaining almost constant thereafter. G4, thus, registers a 33.5% loss in α-helical content at 22.5 μM which corresponds to [G4]/[HSA] ratio of 3 [against a 15% loss by CTAB at 2,250 μM, corresponding to [CTAB]/[HSA] molar ratio of 300]. The gain in the helical content in G4 is again much more significant, i.e. 21% at [G4]/[HSA] molar ratio of 50, compared to 3.5% at [CTAB]/[HSA] ratio of 1,500. The decrease in the α-helical content in G4 as well as CTAB is attributed to the unfolding of the protein whereas the increased α-helix depicts stabilization. The turbidity in the samples did not permit the CD studies to be performed in the concentration range 30–225 μM (Table 2).

The decrease in the helical content is associated with the fact that as the surfactant is added it binds to the protein and thus initiates unfolding (*4*, *28*, *29*). Large amounts of the surfactant molecules are adsorbed on the protein with increasing concentration of the surfactant, forming micelle-like clusters which, in turn, lead the intrachain hydrophobic interactions in the protein to be replaced by the electrostatic repulsive forces between the micellar aggregates, unfold the protein further and thus decrease the α-helical content. The stabilization may be associated with the structural transition of the micelles to a shape with a stronger hydrophobic core as the surfactant concentration increases (*14*).

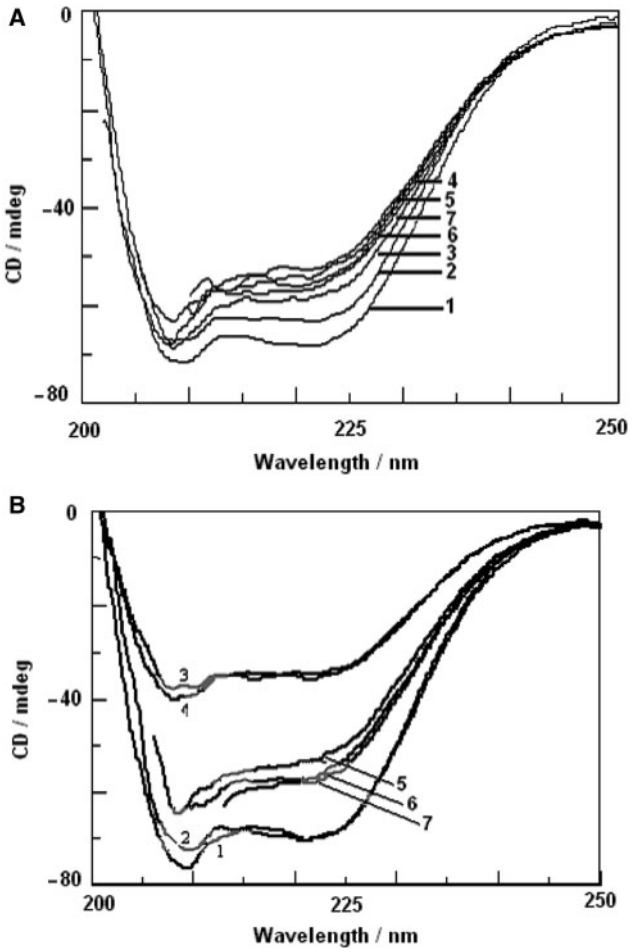

Fig. 2. **Far-UV CD spectra of HSA (7.5 μM) at pH 7, in the native state (1) and in the presence of 300 μM (2), 1,000 μM (3), 2,250 μM (4), 5,250 μM (5), 11,250 μM (6) and 15,000 μM (7) CTAB (2A) and 0 μM (1), 7.5 μM (2), 22.5 μM (3), 30 μM (4) 225 μM (5), 375 μM (6), 750 μM (7) G4 (2B) (temp. 25°C).**

Table 1. **MRE at 222 nm and the percentage of α-helix of HSA at different concentrations of CTAB.**

(CTAB) (μM)	(CTAB)/(HSA)	$-MRE_{222}$	α-helix (%)
0	0	20,000	58.2
300	40	18,114	52
1,000	133	16,608	47
2,250	300	14,942	41.5
5,250	500	15,314	42.8
11,250	1,500	15,971	45
15,000	2,000	15,686	44

The self-association of the surfactant molecules in the aqueous media is highly cooperative and generally starts with the formation of roughly spherical micelles. At higher surfactant concentrations, non-spherical micelles, such as the rod-shaped, may be formed by the surfactant (*54–56*). That the gemini surfactants undergo a structure transition and their hydrodynamic radius increases appreciably with an increase in surfactant concentration has already been studied (*35*). The hydrophobic interactions, due to the stronger hydrophobic microdomain of the gemini surfactant, seem to be enhanced to such an extent that they do not only limit the unfolding but also compress or increase the α-helical content of the protein. In case of the single-chain surfactant, the effect is not significant enough to bring about any noticeable change.

Table 2. **MRE at 222 nm and the percentage of α-helix of HSA at different concentrations of G4.**

(G4) (μM)	(G4)/(HSA)	$-MRE_{222}$	α-helix (%)
0	0	20,000	58.2
7.5	1	19,942	58
22.5	3	9,828	24.7
30	4	10,171	25.8
225	30	15,171	42.3
375	50	16,228	45.8
750	100	16,514	46.7

The results presented clearly show that both the surfactants used (CTAB and G4) lead to a reduction in the secondary structure of the protein upto a particular concentration (because of unfolding of the protein). At high surfactant concentrations, the structure is again induced and stabilization occurs with no further significant change. Although the trend is similar, yet the gemini surfactant is found to be more effective compared to its single chain counterpart.

Near-UV CD—To obtain more information about the structural alterations of HSA, the near-UV CD spectra, which can infer the tertiary structure of HSA (*57–59*), were recorded at different surfactant concentrations. The CD spectra were used to probe the asymmetry of the protein's aromatic amino acid environment.

Figure 3A shows the near-UV CD spectra of HSA in the presence of varying concentrations of CTAB. At 300 μM CTAB an increase in the ellipticity is observed in the entire wavelength range of 250–300 nm (curve 2), compared to the untreated HSA (curve 1), signalling some gain of tertiary structure. At higher surfactant concentrations, i.e. 1,000 μM (curve 3), 2,250 μM (curve 4) and 15,000 μM (curve 5), the ellipticity at 262 nm and 268 nm remains almost unaffected reflecting no significant changes in tertiary structure of the protein. Variations observed in the wavelength range 280–300 nm are ascribed to the changes in the environment of tryptophan residues.

The near UV-CD spectra of the G4–HSA mixed solutions in the wavelength range of 250–300 nm are shown in Fig. 3B. A significant rise in ellipticity compared to the untreated HSA (curve 1) is observed as the protein is treated with 7.5 μM G4 (curve 2) corresponding to a surfactant/protein molar ratio of 1. This is attributed to the presence of two hydrophobic chains in the gemini surfactants which, at these concentrations, make the hydrophobic linkages available between the non-polar residues of the HSA and hence enhance hydrophobicity resulting in increased tertiary structure. A loss in tertiary structure is registered at 22.5 μM G4 (curve 3). The decrease in the tertiary contacts due to decreased α-helical content at this concentration may be responsible for this structure loss. An increase in the tertiary structure is monitored at G4 equal to 375 μM (curve 4) and 750 μM (curve 5). This is associated with the increase

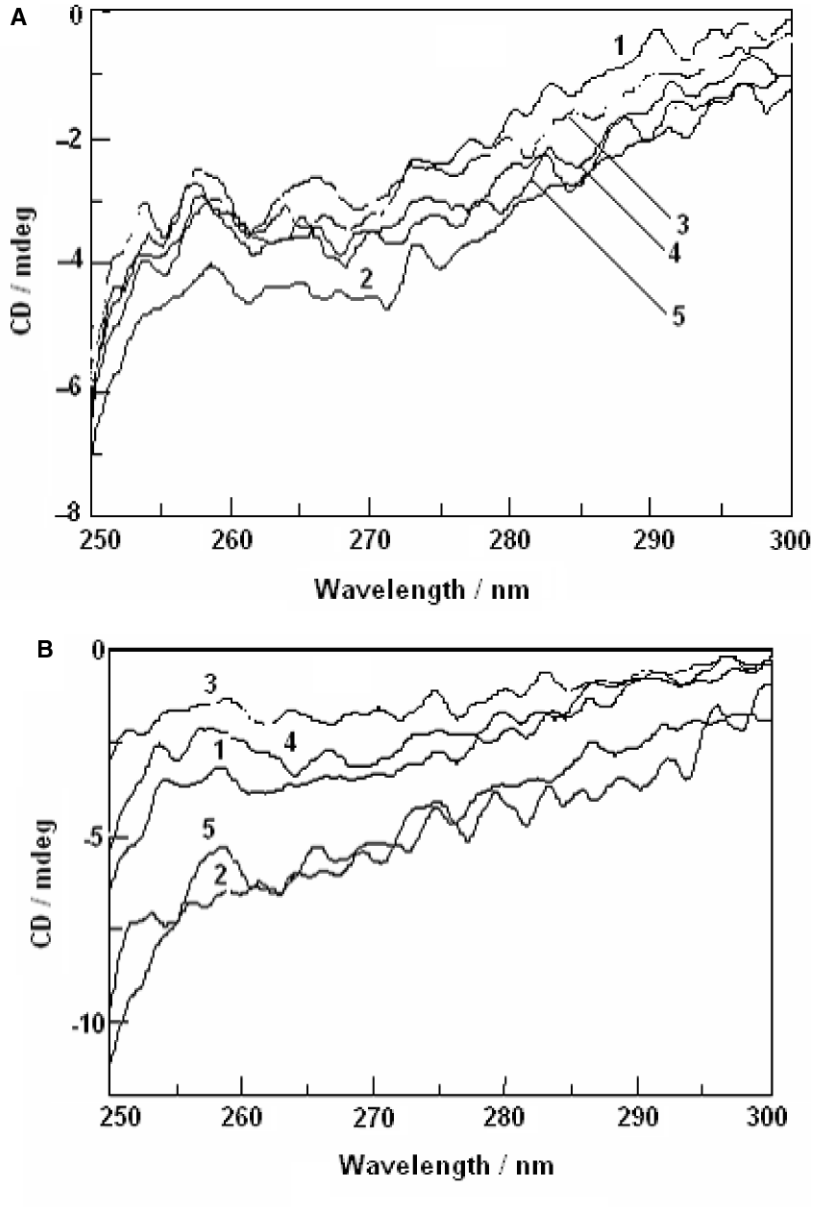

Fig. 3. **Near-UV CD spectra of HSA (7.5 μM) at pH 7 in the native state (1) and in the presence of 300 μM (2), 1,000 μM (3), 5,250 μM (4), 15,000 μM (5) CTAB (3A) and 7.5 μM (2), 22.5 μM (3), 375 μM (4), 750 μM (5) G4 (3B) (temp. 25°C).**

in the hydrophobic interactions as the protein stabilizes. These results are in cognizance with the far UV-CD as well as the aggregation studies and suggest that the gemini surfactant interacts more efficiently with HSA compared to its single chain counterpart, i.e. CTAB.

Intrinsic Fluorescence—The changes in the fluorescence intensities at 340 nm by exciting the protein at 295 nm and 280 nm can be used as a probe for folding/unfolding of proteins (*60*, *61*). A single tryptophanyl residue is present almost at the middle of domain II of HSA (Trp 234) while the eighteen tyrosine residues are distributed among all the domains. The changes in the fluorescence spectra observed by exciting HSA at 295 nm, at which only tryptophan present deep within the HSA molecule is excited, is used to probe the changes in its inner core. On the other hand, at 280 nm both tryptophan and tyrosine residues get excited and this is used to probe changes in their respective microenvironments and provides a picture of the global change in the protein.

In Fig. 4A, changes in the normalized relative fluorescence intensities (RFI) at 340 nm against the increasing concentration of the surfactant (CTAB), as the protein is excited at 280/295 nm, are plotted. Normalized RFI have been calculated by taking the intensity of the untreated protein as 100. The tryptophanyl fluorescence, when HSA is excited at 295 nm, is found to remain almost constant up to 300 μM CTAB (inset of Fig. 4A) corresponding to the CTAB/HSA molar ratio of 40.

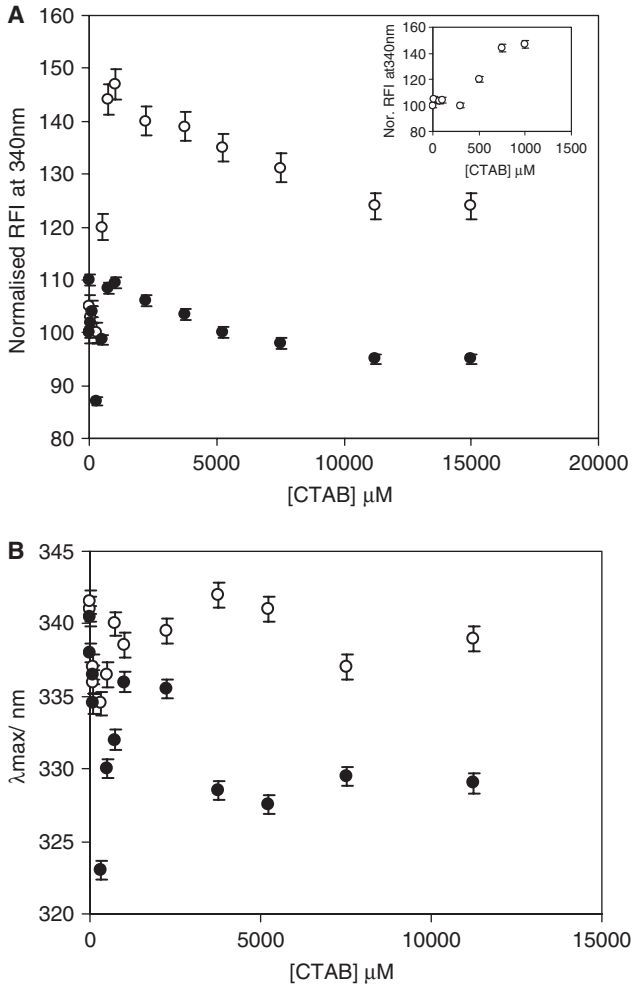

Fig. 4. **(A) Normalized RFI of HSA (7.5 μM) at pH 7 in the presence of CTAB on the basis of fluorescence intensity at 340 nm by exciting at 295 nm (open circle) and 280 nm (filled circle); inset, Normalized RFI of HSA (7.5 μM) at pH 7 in the presence of CTAB on the basis of fluorescence intensity at 340 nm by exciting at 295 nm (open circle).** (B) Change in maximum emission wavelength of CTAB-denatured HSA at 295 nm (open circle) and 280 nm (filled circle) (temp. 25°C).

An increase in RFI is observed in the concentration range 300–1,000 μM ([CTAB]/[HSA] = 133). Beyond 1,000 μM, a decrease in fluorescence intensity is registered which, finally, assumes an almost constant value with further concentration rise. The fluorescence intensity is found to vary similarly when the protein is excited at 280 nm (Fig. 4B). The variations in the wavelength of the emission maximum (λ_{max}), a parameter sensitive to protein conformation (*62*, *63*), is found to follow the intensity changes faithfully. A decrease in λ_{max} or blue shift is observed as RFI decreases and increased RFI is associated with red shift or increased wavelength.

These results predict that CTAB at low concentrations (upto 300 μM) do not influence tryptophanyl fluorescence but the CTAB monomers may quench the tyrosinyl fluorescence and create a hydrophobic environment around these residues resulting in decreased fluorescence intensity and a significant blue shift at the excitation wavelength of 280 nm and no significant changes at 295 nm. This is attributed to the fact that the tryptophan residues are present in the inner core of the HSA while the tyrosine residues are distributed throughout. Thus CTAB as a ligand primarily acts on tyrosine residues. The binding of the surfactant monomers to the inner core leads to the unfolding of the protein and hence exposure of more and more aromatic chromophores to the surface leading to a rise in RFI and a red shift in the concentration range of 300–1,000 μM. The decrease in RFI along with a blue shift beyond 1,000 μM results from the adsorption of the micelles on the protein backbone that gives rise to a hydrophobic environment and leads to fluorescence quenching. The constant value exhibited by the normalized RFI and no significant variations in λ_{max} in the high [CTAB] range is attributed to the fact that the protein backbone is saturated by the micelles at such concentrations and further addition of the surfactant does not alter its environment significantly. These results are in perfect coordination with the binding isotherm suggested for the protein–surfactant interactions (*27*). The variation of the fluorescence intensity (Fig. 4A) is more pronounced at 295 nm than at 280 nm, suggesting that tryptophan is the main contributor of the HSA fluorescence.

Fluorescence measurements, when the protein is excited at 295 nm and 280 nm, were used to monitor the changes in the tertiary structure of HSA induced by its interaction with G4 (Figs 5 and 6). When the excitation wavelength of the protein is set at 280 nm (Fig. 5A), the fluorescence intensity remains almost constant upto 7.5 μM, showing a variation of about three units. On further addition of the surfactant, the intensity exhibits a decreasing trend till the G4 concentration reaches 22.5 μM ([G4]/[HSA] = 3). The variations in the normalised fluorescence intensity at excitation wavelength of 280 nm are perfectly followed by the λ_{max} variations (Fig. 5B), which show a blue shift corresponding to the decreased intensity and a red shift, coupled with the increase in the normalised fluorescence intensity. The decreased fluorescence intensity and the blue shift observed at the surfactant concentration of 22.5 μM suggests that the aromatic chromophores have shifted to a more hydrophobic or apolar environment, possibly because of the formation of micellar aggregates at this concentration. An increase in the fluorescence intensity coupled with a red shift is observed at 30 μM G4 concentration. Insoluble aggregates leading to a very high turbidity limited the fluorescence measurements in the concentration range 30–225 μM. At 225 μM G4 ([G4]/[HSA] = 30), the insoluble aggregates dissociate, supposedly by the stronger hydrophobic domain of the micelles, into soluble complexes and the intensity again shows a rising trend till the surfactant concentration reaches 375 μM ([G4]/[HSA] = 50). The increased intensity may be related to the increase in structure of the protein as suggested by the far-UV CD observations. The normalised fluorescence intensity is found to remain more or less constant beyond the surfactant/protein ratio of 50. Figure 6A presents the spectra demonstrating the fluorescence variations of the HSA–G4 mixed solutions excited at 295 nm containing G4 concentrations of 22.5 μM (curve 2), 225 μM (curve 3), 375 μM (curve 4)

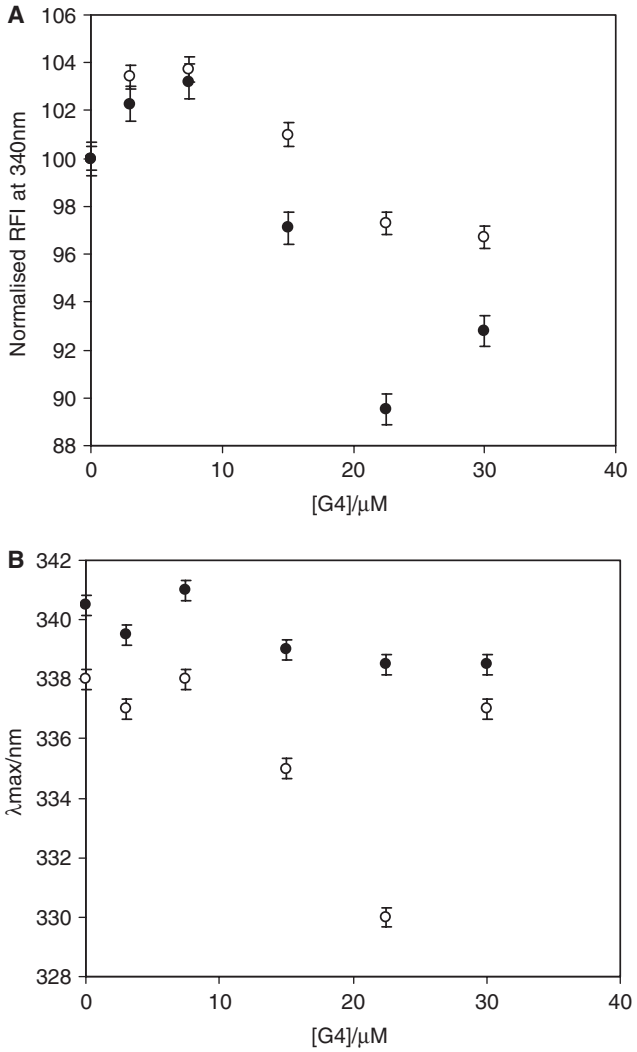

Fig. 5. **(A) Normalized RFI of HSA (7.5 μM) at pH 7 in the presence of G4 on the basis of fluorescence intensity at 340 nm by exciting at 295 nm (open circle) and 280 nm (filled circle).** (B) Change in maximum emission wavelength of G4 (5B) at 295 nm (open circle) and 280 nm (filled circle) (temp. 25°C).

and 750 μM (curve 5). The untreated HSA is demonstrated by curve (*1*). The variations in the fluorescence intensity (Fig. 5A) and λ_{max} (Fig. 5B) at 295 nm show a similar trend with the difference that the fluorescence variations at 280 nm are more significant at low surfactant concentrations that remains almost unchanged at higher concentrations. At higher surfactant concentrations, the fluorescence changes at excitation wavelength of 295 nm are more pronounced (Table 3) for the reasons mentioned above.

These results clearly indicate that the G4 starts interacting with the protein at very low surfactant/protein ratios and the resulting changes culminate or reach the saturation point earlier compared to its single-chain counterpart.

Extrinsic Fluorescence—1-Anilino-8-naphthalene-sulphonate (ANS) is a widely used fluorescent probe known to bind to the hydrophobic patches of

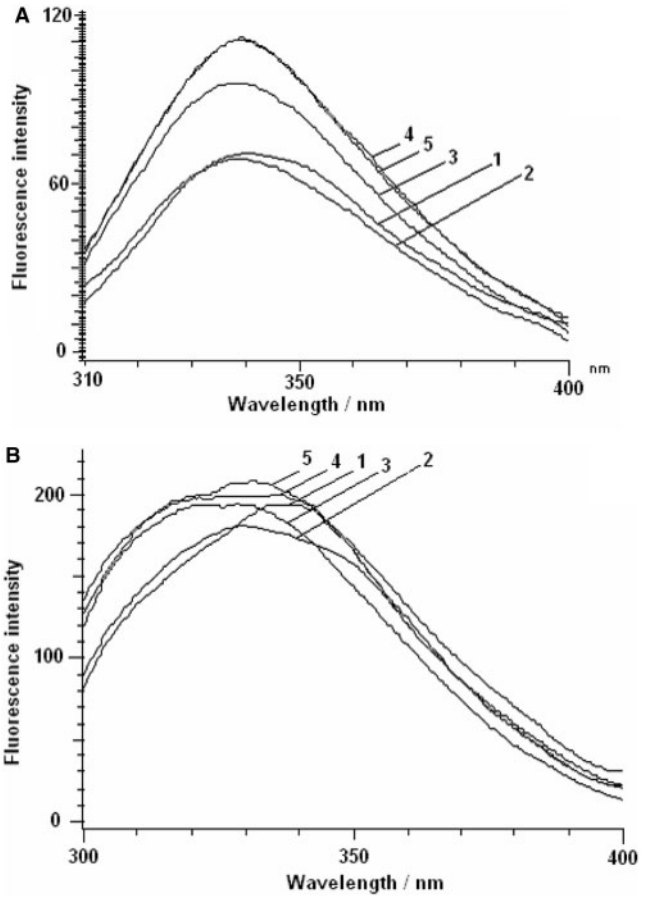

Fig. 6. **Fluorescence spectra of the HSA (7.5 μM) at pH 7 in the native state (1) and in the presence of 22.5 μM (2), 225 μM (3), 375 μM (4), 750 μM (5) G4 when excited at 295 nm (A) and 280 nm (B) (temp. 25°C).**

Table 3. **Normalized RFI of HSA at pH 7 in the presence of different concentrations of G4 on the basis of fluorescence intensity at 340 nm at excitation wavelength of 295 nm or 280 nm.**

		Normalized RFI	
(G4) (μM)	(G4)/(HSA)	(340/295)	(340/280)
0	0	100	100
3	0.4	103.9	102.3
7.5	1	103.7	103.2
15	2	101	97
22.5	3	97	89.5
30	4	97	92.7
225	30	110.6	84.78
375	50	135.6	92.05
525	70	157.7	101.76
750	100	157	102.4

a protein (*64*). There are two different apparent ranges over which ANS binds to the proteins like serum albumins (*65*). One of these is a broad range involving as many as 100 binding sites at pH's below 5, where most of the bound ANS is not fluorescent. In a much narrower range of binding, where ANS is assumed to act as

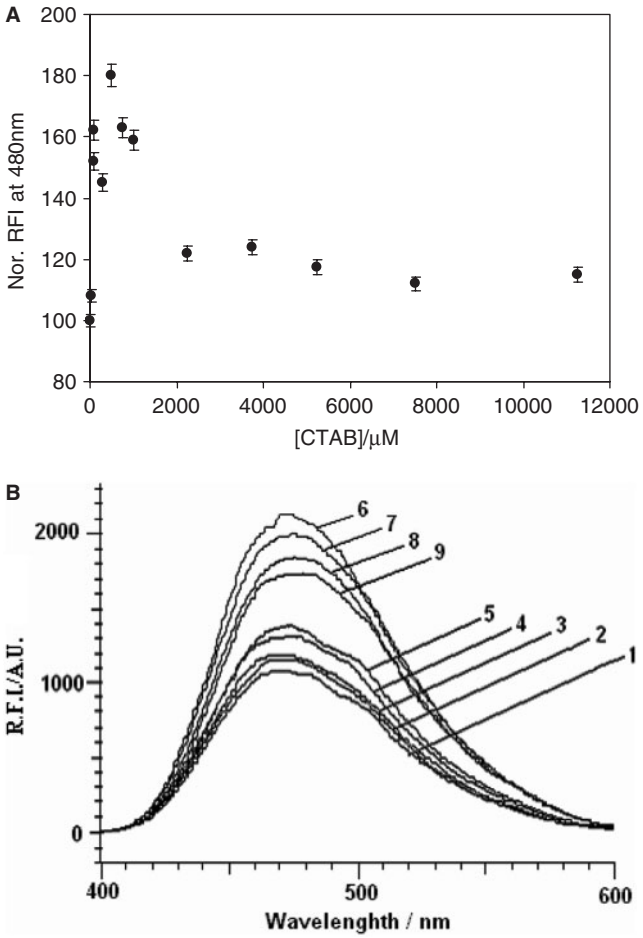

Fig. 7. **(A) Fluorescence intensity at 480 nm of ANS bound HSA (7.5 μM) at pH 7 in the presence of CTAB when excited at 380 nm.** (B) Fluorescence spectra of ANS bound HSA in the presence of varying amounts of G4 when excited at 380 nm [G4] = 0 μM (*1*), 3 μM(*2*), 7.5 μM (*3*), 15 μM (*4*), 22.5 μM (*5*), 225 μM (*6*), 375 μM (*7*), 525 μM (*8*), and 750 μM (*9*) (temp. 25°C).

a hydrophobic probe, ANS may become fluorescent. Five hydrophobic sites have been detected on native serum albumins in the pH range 5–7 (*66*, *67*). The fluorescence exhibited by the native HSA at pH 7 is attributed to the presence of these hydrophobic patches and the variation of the fluorescence intensity can be effectively used to monitor the accessibility of the hydrophobic patches. Bound ANS excites at 380 nm and emits maximally at 480 nm.

Figure 7A depicts the changes in fluorescence intensities at 480 nm with increasing concentrations of CTAB. The initial increase in the ANS binding is due to the co-binding of the surfactant and the probe molecules near the hydrophobic regions of the protein. The proteins exhibit a decrease in ANS binding with increasing surfactant concentrations assuming a constant value finally. The decrease observed is associated with the decrease in the hydrophobic patches as the protein unfolds due to binding of the surfactant molecules resulting in decreased α-helical content. The ANS binding assumes an almost constant value at CTAB equal to 2,250 μM that interestingly coincides with the surfactant concentration beyond which ellipticity and hence the α-helical content does not register any significant variation. Like the far UV-CD results and the intrinsic fluorescence studies ANS binding also follows the binding isotherm suggesting that the protein undergoes conformational changes only up to a particular surfactant concentration after which the protein backbone is saturated with micelles and further addition of the surfactant does not bring about any significant change (*27*).

An increase in ANS binding is observed in the G4 concentration range of 0–22.5 μM (Fig. 7B, curves 1–5). This initial increase in the ANS binding, like in case of CTAB, is associated with the co-binding of the surfactant and the probe molecules near the hydrophobic regions of the protein. The ANS binding could not be monitored in the concentration range 30–225 μM because of the samples turning turbid due to the formation of insoluble aggregates. At 225 μM (*6*), the ANS binding again exhibits a significant increase. This rise coincides with the increase in α-helix in the protein and is attributed to the strong hydrophobic interactions that make the hydrophobic part of the HSA molecule exposed outside while its hydrophilic part is totally buried inside. The binding of ANS to these hydrophobic patches leads to enhancement in the fluorescence intensity. A further decrease of the ANS binding with the increased G4 concentration signals displacement of the probe molecules bound to the protein by the surfactant and their subsequent expulsion in the aqueous phase.

Along with the other spectroscopic tools, the extrinsic fluorescence yet again proves that G4 is more efficient than its conventional counterpart. The peak as well as the decreasing trend in the ANS binding in gemini surfactant is observed much earlier, i.e. at much lower surfactant/protein ratios, compared to that of its single-chain counterpart.

The protein–surfactant interactions, as can be concluded from the above results are very strong in case of gemini surfactants compared to their single chain counterpart. The presence of two charged surfactant headgroups and two non-polar tails in case of the gemini surfactants enhances both the electrostatic as well as hydrophobic forces. This characteristic feature makes them to interact with the protein at comparatively smaller concentrations and these initial interactions trigger changes, owing to the cooperative nature of protein folding/unfolding process (*68*) that makes the gemini surfactant–HSA interactions more significant, resulting in greater unfolding changes in the protein conformation compared to its single chain counterpart. Substantial increase in α-helical content observed in HSA on interacting with G4, compared to the negligible effect in case of CTAB, shows that the hydrophobic forces are enhanced appreciably in case of the gemini surfactant, while the variations are not very significant in case of the single-chain surfactant.

Keeping in view the results presented and the diverse applications of protein-surfactant interactions, it is suggested that the interaction of the geminis with the proteins may add new dimensions to this field. They can be used as solubilizing agents to recover proteins from inclusion bodies. Misfolding and aggregation pose a serious problem to the industrial process of producing

recombinant proteins. Biological systems have sophisticated machinery, the chaperone proteins, for encouraging folding by discouraging aggregation (*69*). Surfactants are efficient folding aids and have proved effective with several proteins (*65*, *68*, *70*). A method, called artificial chaperone-assisted refolding, involving the sequential introduction of a detergent and cyclodextrin and promoting the assembly of protein's native conformation was proposed by Rozema *et al*. (*70–72*). In the first step of this approach the detergent forms a complex with the denatured protein preventing aggregation while in the second step cyclodextrin selectively binds the detergent stripping it from the protein which is then able to refold. The cationic detergent CTAB was found to efficiently refold Xylanase used from alkalophilic thermophilic bacillus (*73*). Since the gemini surfactant has more affinity for the protein then its conventional counterpart, it may be used as an efficient and inexpensive folding catalyst that acts like chaperone and helps in the optimization of the refolding process. The gemini surfactant, because of stronger electrostatic and hydrophobic forces, may capture the denatured protein at much lower concentration compared to the single-chain surfactant in the first step of the artificial chaperone protocol and hence inhibit aggregation. Since the slow removal of detergent from the protein is deleterious to proper refolding, it may be stripped by cyclodextrin more rapidly and thus facilitate the second step.

Certain surfactants have been found to enhance the absorption of drugs from the surface of skin or from mucous membrane but the amounts of the surfactants have been found to show irritating properties and the use of low surfactant concentrations has been suggested (*74*). From the present study we conclude that the gemini surfactants may prove to be more efficient and supposedly may act at lower concentrations compared to their single-chain counterparts.

CONCLUSIONS

We have tracked the comparative interaction of HSA with the cationic single-chain surfactant CTAB and its gemini counterpart with spacer $-(CH_2)_4-$ using well-recognized spectroscopic techniques. The results arrived at made it amply clear that the gemini surfactant G4 affects the conformation of HSA much more significantly than its single-chain counterpart CTAB. The results are attributed to the architecture of the gemini surfactant that confer it with unique characteristics such as much lower cmc, special aggregate morphology, and a very strong hydrophobic microdomain (*28–33*). These properties enable the gemini surfactant to interact with the protein at much lower concentrations resulting in unfolding and also leads to more substantial stabilization at higher concentrations compared to its single chain counterpart. We wait, with great excitement, to see how the present work is utilized to investigate the potential of the gemini surfactants in various areas especially in drug delivery, as artificial chaperones, and as solubilizing agents to recover proteins from insoluble inclusion bodies.

CONFLICT OF INTEREST

None declared.

REFERENCES

1. Guo, X.H., Zhao, N.M., Chen, S.H., and Teixeira, J. (1990) Small angle neutron scattering study of the structure of protein/detergent complexes. *Biopolymers* **29**, 335–346
2. Tanford, C. (1980) *The Hydrophobic Effect: Formation of Micelles and Biological Membranes*, 2nd edn, Chapter 14, pp. 123, Wiley Interscience, New York
3. Anson, M.L. (1939) The denaturation of proteins by detergents and bile salts. *Science* **90**, 256–257
4. Jones, M.N. (1975) A theoretical approach to the binding of amphiphilic molecules to globular proteins. *Biochem. J.* **151**, 109–114
5. Gull, N., Sen, P., Kabir-ud-Din, and Khan, R.H. (2007) Effect of physiological concentration of urea on the conformation of human serum albumin. *J. Biochem.* **141**, 261–268
6. Gull, N., Kumar, S., Ahmed, B., Khan, R.H., and Kabir-ud-Din (2006) Influence of urea additives on micellar morphology/protein conformation. *Colloids Surf. B.* **51**, 10–15
7. Pace, C.N. (1990) Measuring and increasing protein stability. *TIBECH.* **8**, 93–98
8. Rao, P.F. and Takagi, T. (1989) Reassessment of the viscosity behaviour of sodium dodecyl sulphate–protein polypeptide complexes. *J. Biochem.* **106**, 365–371
9. Turro, N.J., Lei, X.G., Ananthapadmanabhan, K.P., and Aronson, M. (1995) Spectroscopic probe analysis of protein–surfactant interactions: the BSA/SDS system. *Langmuir* **11**, 2525–2533
10. Greener, J., Contestable, B.A., and Bale, M.D. (1987) Interaction of anionic surfactants with gelatin: viscosity effects. *Macromolecules* **20**, 2490–2498
11. Shinagawa, S., Kameyama, K., and Takagi, T. (1993) Effect of salt concentration of buffer on the binding of sodium dodecyl sulphate and on the viscosity behavior of the protein polypeptide derived from bovine serum albumin in the presence of the surfactant. *Biochim. Biophys. Acta.* **1161**, 79–84
12. Wright, A.K., Thompson, M.R., and Miller, R.L. (1975) A Study of protein–sodium dodecyl sulphate complexes by transient electric birefringence. *Biochemistry* **14**, 3224–3228
13. Galemo, E.L., Silva, C.H., Imasato, H., and Tabak, M. (2002) Interaction of bovine (BSA) and human (HSA) with ionic surfactants: Spectroscopy and modeling. *Biochim. Biophys. Acta.* **1594**, 84–99
14. Sun, C., Yang, J., Wu, X., Huang, X., Wang, F., and Liuh, S. (2005) Unfolding and refolding of bovine serum albumin induced by cetylpyridinium bromide. *Biophys. J.* **88**, 3518–3524
15. Nnanna, I.A. and Xia, J. (2001) *Protein Based Surfactants; Surfactant Science Series* Vol. 101, Marcel Dekker, New York
16. La Mesa, C. (2005) Polymer–surfactant and protein–surfactant interactions. *J. Colloid Interface Sci.* **286**, 148–157
17. Crieghton, T.E. (1991) Stability of folded conformations. *Curr. Opin. Struct. Biol.* **1**, 5–16
18. Hvidt, A. and Westh, P. (1998) Different views on the stability of protein conformations, and hydrophobic effects. *J. Solution Chem.* **27**, 395–402
19. Helenius, A. and Simons, K. (1975) Solubilization of membranes by detergents. *Biochim. Biophys. Acta.* **415**, 29–79
20. Jones, O.T., Earnest, J.P., and McNamee, M.G. (1987) Solubilizaton and reconstruction of biological membranes in *Biological Membranes: A Practical Approach.* (Findley, J.B.C. and Evance, W.H., eds.) pp. 139–177, IRL Press, Oxford

21. Moore, P.N., Puwada, S., and Blankschtein, D. (2003) Role of the surfactant polar head structure in protein–surfactant complexation: zein protein solubilization by SDS and by SDS/$C_{12}E_n$ surfactant solutions. *Langmuir* **19**, 1009–1016
22. Kelley, D. and McClements, D.J. (2003) Interaction of bovine serum albumin with ionic surfactants in aqueous solutions. *Food Hydrocolloids* **17**, 73–85
23. Valster, A., Brown, W., and Almgren, M. (1999) The lysozyme-sodium dodecyl sulfate system studied by dynamic and static light scattering. *Langmuir* **15**, 2366–2374
24. Honda, C., Kamizono, H., Matsumoto, K., and Endo, K. (2004) Studies on bovine serum albumin–sodium dodecyl sulfate complexes using pyrene fluorescence probe and 5-doxylstearic acid spin probe. *J. Colloid Interface Sci.* **278**, 310–317
25. Santos, S.F., Zenette, D., Fischer, H., and Itri, R. (2003) A systematic study of bovine serum albumin (BSA) and sodium dodecyl sulfate (SDS) interactions by surface tension and small angle X-ray scattering. *J. Colloid Interface Sci.* **262**, 400–408
26. Wangsakan, A., Chinachoti, P., and McClements, D.J. (2004) Effect of surfactant type on surfactant maltodextrin interactions: Isothermal titration calorimetry, surface tensiometry and ultrasonic velocimetry study. *Langmuir* **20**, 3913–3919
27. Few, A.V., Ottewill, R.H., and Parreira, H.C. (1955) The interaction between bovine plasma albumin and dodecyltrimethylammonium bromide. *Biophys. Biochim. Acta.* **18**, 136–137
28. Nozaki, Y., Reynolds, J.A., and Tanford, C. (1974) The interaction of a cationic detergent with bovine serum albumin and other proteins. *J. Biol. Chem.* **249**, 4452–4459
29. Ray, S. and Chakrabarti, A. (2003) Erythroid Spectrin in miceller detergents. *Cell Motil. Cytoskeleton* **54**, 16–28
30. McCoy, M.A. and Wyss, D.F. (2002) Structures of protein–protein complexes are docked using only NMR restraints from residual dipolar coupling and chemical shift perturbations. *J. Am. Chem. Soc.* **124**, 2104–2105
31. Menger, F. M and Littau, C.A. (1993) Gemini Surfactants: a new class of self-assembling molecules. A. *J. Am. Chem. Soc.* **115**, 10083–10090
32. Zana, R. and Xia, J. (2004) *Gemini Surfactants* (Zana, R. and Xia, J., eds.) Marcel Dekker, New York
33. Rosen, M.J. (1993) Geminis: a new generation of surfactants. *Chemtech.* **23**, 30–33
34. Zana, R. (2002) Dimeric and oligomeric surfactants. Behavior at interface and in aqueous solution: a review. *Adv. Colloid Interface Sci.* **97**, 205–253
35. Siddiqui, U.S., Ghosh, G., and Kabir-ud-Din (2006) Dynamic light scattering studies of additive effects on the microstructure of aqueous gemini micelles. *Langmuir* **22**, 9874–9878
36. Kabir-ud-Din, Siddiqui, U.S., Kumar, S., and Dar, A.A. (2006) Micellization of monomeric and dimeric (Gemini) surfactants in polar non-aqueous water mixed solvent. *Colloid Polym. Sci.* **284**, 807–812
37. Li, Y., Wang, X., and Wang, Y. (2006) Comparative studies on interactions of bovine serum albumin with cationic Gemini and single chain surfactants. *J. Phys. Chem. B* **110**, 8499
38. Pi, Y., Shang, Y., Peng, C., Liu, H., Hu, Y., and Jiang, J. (2006) Interaction between bovine serum albumin and Gemini surfactant alkanediyl-alpha, omega-bis(dimethyldodecyl-ammonium bromide). *Biopolymers* **83**, 243–249
39. Wu, D., Xu, G., Feng, Y., and Li, Y. (2007) Aggregation behaviors of gelatin with cationic gemini surfactant at air/water interface. *Int. J. Biol. Macromol.* **40**, 345–50
40. Wu, D., Xu, G., Sun, Y., Zhang, H., Mao, H., and Feng, Y. (2007) Interaction between proteins and Gemini surfactant. *Biomacromolecules* **8**, 708–712
41. He, X.M. and Carter, D.C. (1992) Atomic structure and chemistry of human serum albumin. *Nature* **358**, 209–215
42. Peters, T., Jr. (1985) Serum albumin. *Adv. Protein Chem.* **37**, 161–245
43. Carter, D.C. and Ho, J.X. (1994) Structure of serum albumin. *Adv. Protein Chem.* **45**, 153–203
44. Vijai, K. K and Forster, J.F. (1967) The amphoteric behavior of bovine plasma albumin: Evidence for masked carboxylate groups in the native protein. *Biochemistry* **6**, 1152–1159
45. Peters, T., Jr. (1996) *All About Albumin Biochemistry, Genetics and Medical Applications*, Academic Press, California
46. Wallevik, K. (1973) Reversible denaturation of human serum albumin by pH, temperature, and guanidine hydrochloride followed by optical rotation. *J. Biol. Chem.* **248**, 2650–2655
47. Lowry, O.H., Rosebrough, N.J., Farr, A.L., and Randall, R.J. (1951) Protein measurements with the folin phenol reagent. *J. Biol. Chem.* **193**, 265–275
48. Chen, Y.H., Yang, J.T., and Martinez, H. (1972) Fluorescence stopped flow study of relaxation process in the binding of bilirubin to serum albumins. *Biochemistry* **11**, 4120–4131
49. Dubin, P.L., Vea, M.E.Y., Fallon, M.A., Thé, S.S., Rigsbee, D.R., and Gan, L.M. (1990) Higher order association in polyelectrolyte-micelle complexes. *Langmuir* **6**, 1422–1427
50. Sudbeck, E.A., Dubin, P.L., Curran, M.E., and Skelton, J. (1991) Dye solubilization in polyelectrolyte–micelle complexes. *J. Colloid Interface Sci.* **142**, 512–517
51. Xia, J., Zhang, H., Rigsbee, D.R., Dubin, P.L., and Shaikh, T. (1993) Structural Elucidation of soluble polylectrolyte–micelle complexes: intra- Vs interpolymer association. *Macromolecules* **26**, 2759–2766
52. Ananthapadhmanabhan, K.P. (1993) *Interaction of Surfactant with Polymers and Proteins* (Goddard, E.D. and Ananthapadhmanabhan, K.P., eds.) CRC Press, Boca Raton, FL
53. Corbin, J., Methlot, N., Wang, H.H., Baenziger, J.E., and Blanton, M.P. (1998) Secondary structure analysis of individual transmembrane segments of the nicotinic acetylcholine receptor by circular dichroism and fourier transform infrared spectroscopy. *J. Biol. Chem.* **273**, 771–777
54. Birdi, K.S. (1977) *Micellization, Solubilization and Microemulsion.* (Mittal, K.L., ed.) p. 151, Plenum Press, New York
55. Ekwall, P., Mandell, L., and Solyom, P. (1971) The Aqueous cetyltrimethylammonium bromide solutions. *J. Colloid Interface Sci.* **35**, 519–528
56. Imae, T., Kamiya, R., and Ikeda, S. (1985) Formation of spherical and rod-like micelles of cetyltrimethylammonium bromide in aqueous NaBr solutions. *J. Colloid Interface Sci.* **108**, 215–225
57. Dockal, M., Carter, D.C., and Ruker, F. (2000) Conformational transitions of the three recombinant domains of human serum albumin depending on pH. *J. Biol. Chem.* **275**, 3042–3050
58. Kelly, S.M. and Price, N.C. (1997) The application of circular dichroism to studies of protein folding and unfolding. *Biochim. Biophys. Acta.* **1338**, 161–185
59. Price, N.C. (2000) Conformational issues in the characterization of proteins. *Biotechnol. Appl. Biochem.* **31**, 29–40
60. Chen, Y. and Barkley, M.D. (1998) Towards understanding tryptophanyl fluorescence in proteins. *Biochemistry* **37**, 9976–9982
61. Pace, C.N., Vajdos, F., Fee, L., Grimsley, G., and Gray, T. (1995) How to measure and predict the molar absorption coefficient of a protein. *Protein Sci.* **4**, 2411–2423
62. Ghisla, S., Massey, V., Lhoste, J.M., and Mayhew, S.G. (1974) Fluorescence and optical characteristics of reduced flavines and flavoproteins. *Biochemistry* **13**, 589–597

63. Deep, S. and Ahluwalia, J.C. (2001) Interaction of bovine serum albumin with anionic surfactants. *Phys. Chem. Chem. Phys.* **3**, 4583–4591
64. Stryer, L. (1965) The interaction n of naphthalene dye with apohemoglobin. A fluorescent probe of non-polar binding sites. *J. Mol. Biol.* **13**, 482–495
65. Matulis, D. and Lovrien, R (1998) 1-Anilino-8-Naphthalene sulfonate anion-protein binding depends on ion pair formation. *Biophys. J.* **74**, 422–429
66. Slavik, J. (1982) Anilinonaphthalene sulfonate as a probe of membrane composition and function. *Biochim. Biophys. Acta.* **694**, 1–25
67. Daniel, E. and Weber, G. (1966) Cooperative effects in binding by bovine serum albumin. The binding of 1-Anilino-8-Naphthalene sulfonate. Fluorimetric titrations. *Biochemistry* **5**, 1893–1900
68. Chandler, D. (2002) Hydrophobicity: two faces of water. *Nature* **417**, 491
69. Harlt, F.U. (1996) Molecular chaperone in cellular protein folding. *Nature* **381**, 571–580
70. Rozema, D. and Gellman, S.H. (1995) Artificial chaperones: protein refolding via sequential use of detergent and cyclodextrin. *J. Am. Chem. Soc.* **117**, 2373–2374
71. Rozema, D. and Gellman, S.H. (1996) Artificial chaperone-assisted refolding of carbonic anhydrase B. *J. Biol. Chem.* **271**, 3478–3487
72. Rozema, D. and Gellman, S.H. (1996) Artificial chaperone-assisted refolding of denatured-reduced lysozyme: modulation of the competition between renaturation and aggregation. *Biochemistry* **35**, 15760–15771
73. Nath, D. and Rao, M. (2001) Artificial chaperone mediated refolding of xylanase from an alkalophilic thermophilic bacillus sp. *Eur. J. Biochem.* **268**, 5471–5478
74. Gloxhuber, C. and Kunstler, K. (1992) *Anionic Surfactants: Biochemistry, Toxicology, Dermatology* (Gloxhuber, C., ed.) Marcel Dekker, New York